

6.2 NFT of ^{11}Be : one-particle transfer in halo nuclei.
The nucleus ^{11}Be , constitutes an example of one-neutron halo system, namely a halo neutron outside the $N=6$ closed shell resulting from the phenomenon of parity inversion.^{*)}

(B) - (B) pp. 5+6 last version of paper Hawking

+ Fig. 1 → 6.2.1

and Fig. 2 → 6.2.2

of the same paper.

In what follows we elaborate on some of the details of the NFT ($r+s$) calculations^{**) at the basis of the above results.}

(C) - (C) pp. 1-4 Latest version PRL
 ^{11}Be .

6.3 Summary

In Figure 6.3.1 a "complete" (NFT)_{ren} ($s+r$) description of the single-neutron outside closed shell halo nucleus ^{11}Be in terms

**) Barranco et al (2017)

*) This nucleus has been extensively studied both experimentally [1-8] and theoretically [9-25].
For

Barranco et al (2017)

paper submitted to PRL

the references 1-25 are from this paper.

of the reactions $^2\text{H}(^{10}\text{Be}, ^{11}\text{Be})^7\text{H}$ populating the $\frac{1}{2}^+, \frac{1}{2}^-$ and $\frac{5}{2}^+$ states and the $^7\text{H}(^{11}\text{Be}, ^{10}\text{Be})^2\text{H}$ populating the 2^+ mode, the E1-transition between the parity inverted states $\frac{1}{2}^+, \frac{1}{2}^-$ and the isotopic shift of the charged radius of ^{10}Be , are displayed in comparison with the experimental findings. There are in all four parameters entering the calculation (depth, radius, diffusivity and R-mass ($m_{RD}=0.7\text{ m}$), bare potential), and four empirical inputs (energy and deformation parameter of the quadrupole mode of ^{10}Be , energy of the octupole vibration and of the pair removal mode).

Repeating the last paragraph of sect. 1.10 ~~one can again state that,~~ in a very real sense, this is a nucleus.

— italics

3

inducing the nuclear reaction and of the resulting outgoing particles, the other term being associated with the reaction Q -value^{Note1}. While the outcome of the γ -coincidence experiment (related to the $h\nu_2$ term in (3)) can be taken for granted, its actual implementation in processes based on inverse kinematics like the one under consideration, is technically quite trying. Be as it may, the fact that the calculated absolute transfer cross sections provide an overall account of the experimental findings [14, 17] gives direct insight into the soundness of the (renormalised) NFT picture of the nuclear vacuum state has.

Let us now return to Fig. 1(II). The bare properties of an odd nucleon moving around the core (Fig. 1(II)(b)) get modified through Pauli principle (Fig. 1(II)(c)) and through the associated clothing process resulting from time ordering (Fig. 1(II)(d)). Within the scenario of quantum electrodynamic (QED) where Feynman diagrams were developed and in keeping with the symmetry existing between positron and electron phase spaces, N- and I-like processes (Figs. 1(II)(c) and (d)) are operative on equal footing. Observation of any of the associated virtual processes clothing the electron through the action of an external field (e.g. Fig. 1(III)(b)), carries similar information concerning the presence of vacuum fluctuations as, for example, the process (a) of Fig. 1(III) does. Because of spatial quantisation, finite nuclei display an asymmetry between occupied and empty states. As a consequence process (c) of Fig. 1(II) may be allowed and not process (d), or viceversa. This is particularly true for light nuclei, for example ^{11}Be .

B

In the core of ^{11}Be , namely $^{10}_4\text{Be}_6$, six neutrons occupy the $1s_{1/2}$ and $1p_{3/2}$ levels (Fig. 2). The dominant ZPF is of quadrupole type, the main component being associated with the $((p_{1/2}, p_{3/2}^{-1}) \otimes 2^+)_0+$ ZPF (Fig. 8(II)(a)). Because $\epsilon_{p1/2} - \epsilon_{p3/2} \approx 3.8$ MeV and $\hbar\omega_{2+} = 3.368$ MeV, the largest amplitude of the quadrupole mode is associated with particle-hole excitation $(p_{1/2}, p_{3/2}^{-1})_{2+}$. The repulsion due to Pauli (Fig. 2 inset (A)) is ≈ 2.8 MeV. The clothing of the $2s_{1/2}$ bare level by the quadrupole mode (Fig. 2 inset (B), see also Fig. 8(I)(a)) makes it heavier, lowering its energy by almost 1 MeV (710 keV). The result of the two processes mentioned above is parity inversion (Fig. 2) and the appearance of the $N = 6$

6.1.1

^{Note1} In a recent paper by Hawking and coworkers [15], Hawking radiation is extended to encompass a low-energy version of photons, e.g. hypothetical particles known as gravitons. Centered around the question of whether the outflowing particles would have or not completely random properties, it can be posited that if the vacuum has different states, one can transfer information into the radiation without putting energy at the horizon. If one were to make any parallel between the horizon of black holes and the external fields, which certainly is not the point of the present paper, one could argue that one has to put energy at the horizon (see [3]). In the nuclear cases under discussion, one knows its value: $\Delta mc^2 + \Delta T$.

(4)

6.2.1

new magic number together with the melting away of the $N = 8$ standard one. In a similar way in which the Lamb shift (Fig. 6, inset C) provides a measure of the fluctuations of the QED vacuum (see [16], p. 451), parity inversion measures ZPF of the nuclear vacuum (ground) state. In this last case further information can be obtained as compared with the atomic case, through particle transfer reactions.

Interpreting the arrowed lines of Fig. 1(III) as an electron and a positron, the wavy curve as a photon and the external field (cross + dashed line) as the event horizon of a black hole one has a Feynman representation of Hawking radiation. A nuclear analogue of such radiation, to the extent that one considers only the wavy line and the detector click, is provided by graph (b) of Fig. 1(III), if one interprets the arrowed line as a nucleon, the wavy line as a nuclear vibration and the external field as a nucleon pickup process.

A concrete example of the above parlance is provided by the one neutron pickup reaction of the single-halo valence nucleon of ^{11}Be , leading to the population of the low-lying quadrupole, first excited (vibrational) state of the core ^{10}Be , as shown in Fig. 3(I)(b) (see also Fig. 3(II) in relation with the spontaneous ^{Note 1} γ -decay of the 2^+ state, in coincidence with the reaction process). Light nuclei at the drip line provide another paradigmatic example of parity inversion and of a nuclear analogue, again in the sense of a virtual process becoming real through the action of an external field, of Hawking radiation: the nucleus is ^{11}Li , the process in question being $^1\text{H}(^{11}\text{Li}, ^9\text{Li}(1/2^-, 2.69 \text{ MeV}))^3\text{H}$ (Fig. 4).

The vacuum state of a quantal system contains, through zero point fluctuations, virtual information concerning the particles (elementary modes of excitation in the case of a many-body system) and of their interactions (interweaving). To bring this information to the detector, one needs to intervene the virtual states with external fields which share the properties one wants to observe. One-particle transfer to learn about the clothing of the motion of nucleons in nuclei, Cooper pair transfer to learn about the mechanisms by which gauge invariance can be violated.

In a similar way in which the Lamb shift provided a definitive answer to Rabi's question of whether the polarisation of a QED vacuum could be measured [16], parity inversion provides a definitive answer to the central role collective vibrations play in the clothing processes of valence nuclear motion, as testified by the Hawking-like radiation observed in

6.2.2

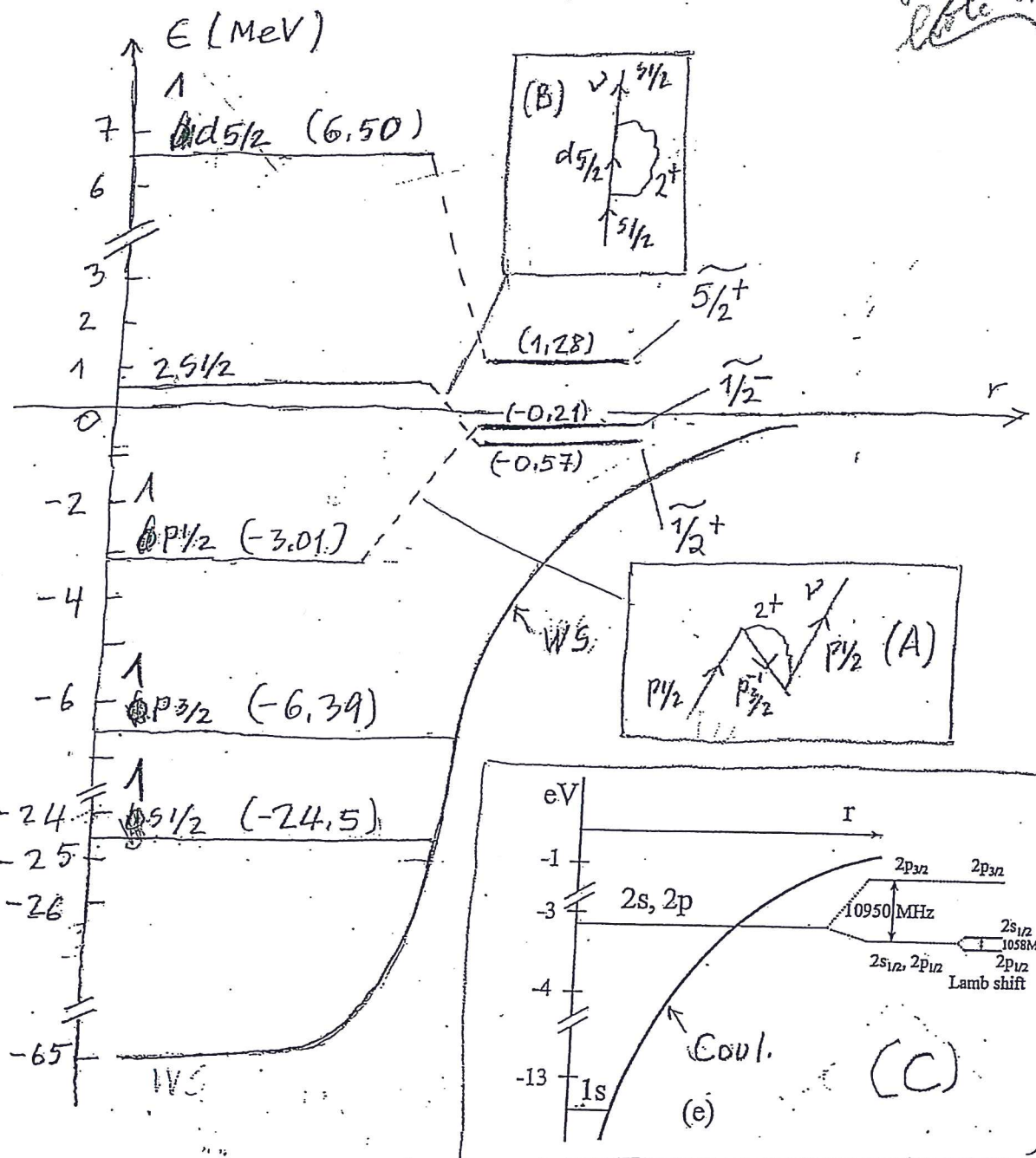
B

^{Note 1} Spontaneous γ -decay is a direct consequence of the ZPF of the nuclear vacuum (through its proton component) due to the presence of the ZPF of the electromagnetic field.

-
- [1] S.W. Hawking, *Particle creation by black holes*, Commun. Math. Phys. **43**, 199 (1975)
- [2] J. Steinhauer *Observation of quantum Hawking radiation and its entanglement in an analogue black hole*, Nature Phys. **12**, 959 (2016)
- [3] D. Castelvecchi, *Artificial black hole creates its own version of Hawking radiation*, Nature, 536 (2016) 258
- [4] S. Schweber, *QED and the men who made it: Dyson, Feynman, Schwinger and Tomonaga*, Princeton University Press (1994)
- [5] D.R. Bes, G.G. Dussel, R.A. Broglia, R. Liotta and B.R. Mottelson, *Nuclear field theory as a method of treating the problem of over completeness in descriptions involving elementary modes of both quasiparticles and collective type*, Phys. Lett. B **52**, 253 (1974)
- [6] P.F. Bortignon, R.A. Broglia, D.R.Bes and R. Liotta, *Nuclear Field Theory*, Phys. Rep. **30C** (1977) 305
- [7] D.R. Bes, G.G. Dussel, R.P.J. Perazzo and H.M.Sofía, *The renormalization of single-particle states in Nuclear Field Theory*, Nucl. Phys. A **293**, 350 (1977)
- [8] R.A. Broglia, P.F. Bortignon, F. Barranco, E. Vigezzi, A. Idini and G. Potel, *Unified description of structure and reactions: implementing the nuclear field theory program*, Physica Scripta **91**, 063012 (2016)
- [9] I. Tanihata, H. Savajols and R. Kanungo, *Recent experimental progress in nuclear halo structure studies*, Prog. Part. Nucl. Phys. **68**,215 (2013)
- [10] N. Keeley, N. Alamanos and V. Lapoux, *Comprehensive analysis method for (d,p) stripping reactions*, Phys. Rev. C**69** (2004) 064604
- [11] S. Shimoura
- [12] J.S. Winfield *et al.*, *Single-neutron transfer from ^{11}Be via the (p,d) reaction with a radioactive beam*, Nucl. Phys. A**683** 48 (2001)
- [13] I. Tanihata et al, *Measurement of the two-halo neutron transfer reaction $^1\text{H}(^{11}\text{Li}, ^9\text{Li})^3\text{H}$ at $3A \text{ MeV}$* , Phys. Rev. Lett. **100**, 192502 (2008)
- [14] G. Potel, F. Barranco, E. Vigezzi and R.A. Broglia, *Evidence for phonon mediated pairing interaction in the halo of the nucleus ^{11}Li* , Phys. Rev. Lett. **105** (2010) 172502
- [15] S.W. Hawking et al, *Soft hair on black holes*, Phys. Rev. Lett. **116** (2016) 231301

(6)

- [16] A. Pais, *Inward bound*, Oxford University Press, Oxford (1986)
- [17] F. Barranco, G. Potel, R.A. Broglia and E. Vigezzi , *Structure and reactions of ^{11}Be : many-body basis for single-neutron halo*, to be published
- [18] C. Bachelet et al, *Mass measurement of short-lived halo nuclides*, EPJ A 25 (2005) 31
- [19] S. Baroni, M. Armati, F. Barranco, R.A. Broglia, G. Colò, G. Gori and E. Vigezzi, *Correlation energy contribution to nuclear masses*, J. Phys. G 30, 1353 (2004)
- [20] H.B.G. Casimir, *On the interaction between two perfectly conducting plates*, Proc. Kon. Ned. Akad. Wetensch. B 51 (1948) 793
- [21] H.B.G. Casimir, *The influence of retardation on the London-van der Waals forces*, Phys. Rev. 73 (1948) 360
- [22] J. N. Israelchvili, *Intermolecular and surface forces*, Academic Press, New York (1985), p. 65
- [23] L. Pauling and E.B. Wilson, *Quantum mechanics*, Dover, New York (1963), p. 383
- [24] F. London, *Zur Theorie der Systematik der Molekularkräfte*, Z. Phys. 63 (1930) 245
- [25] H. Kawabara, *Hawking radiation of black holes*, 1/12/2014
- [26] R.A. Broglia and Aa. Winther, *Heavy ion reactions*, Westview Press, Cambridge, MA (2004)
- [27] G. Potel, A. Idini, F. Barranco, E. Vigezzi and R.A: Broglia, *Cooper pair transfer* , Rep. Prog. Phys. 76 (2013) 106301
- [28] A. Bohr and B.R. Mottelson, *Nuclear structure*, Vol.II, Benjamin (1975)
- [29] B.R. Holstein, *Weak interaction in nuclei*, Princeton University Press, New Jersey (1989)
- [30] W. Lamb and R. Retherford, *Fine structure of the hydrogen atom by a microwave method*, Phys. Rev. 72 (1947) 241
- [31] N.M. Kroll and W.E. Lamb, *On the self-energy of a bound electron*, Phys. Rev. 75 (1949) 388



Caption
Fig. 13

Fig. 1

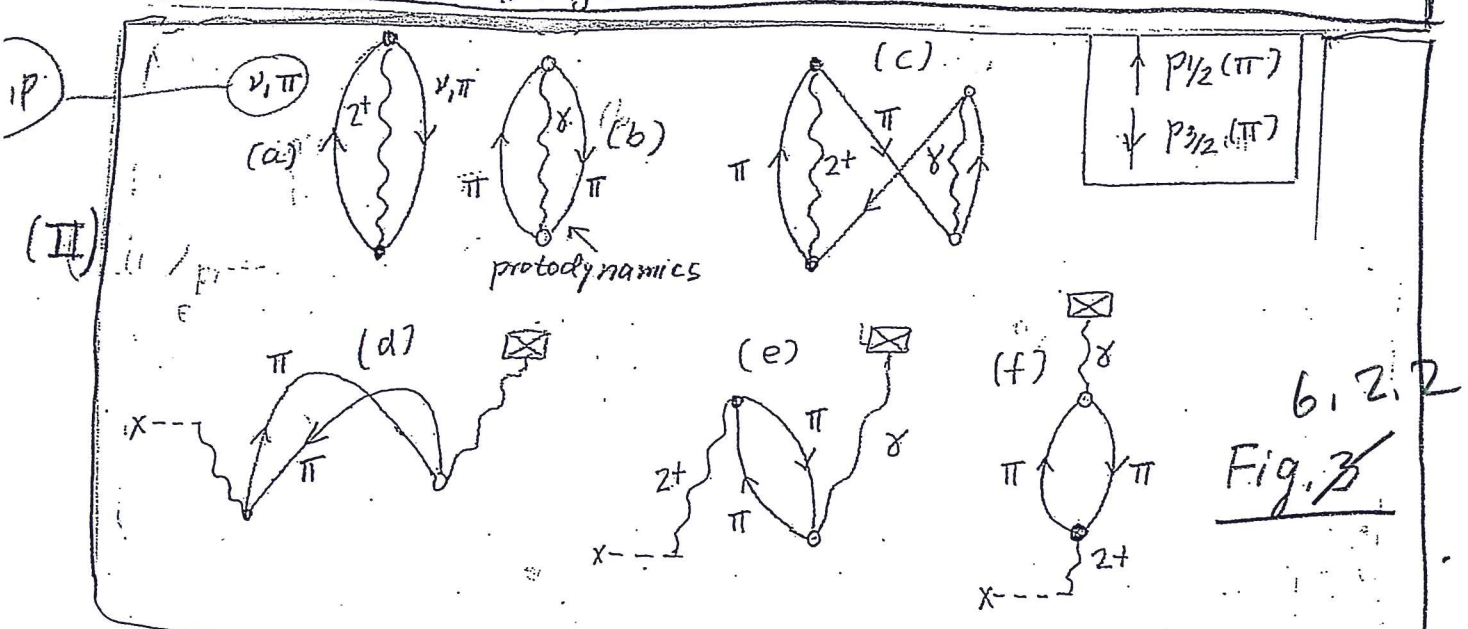
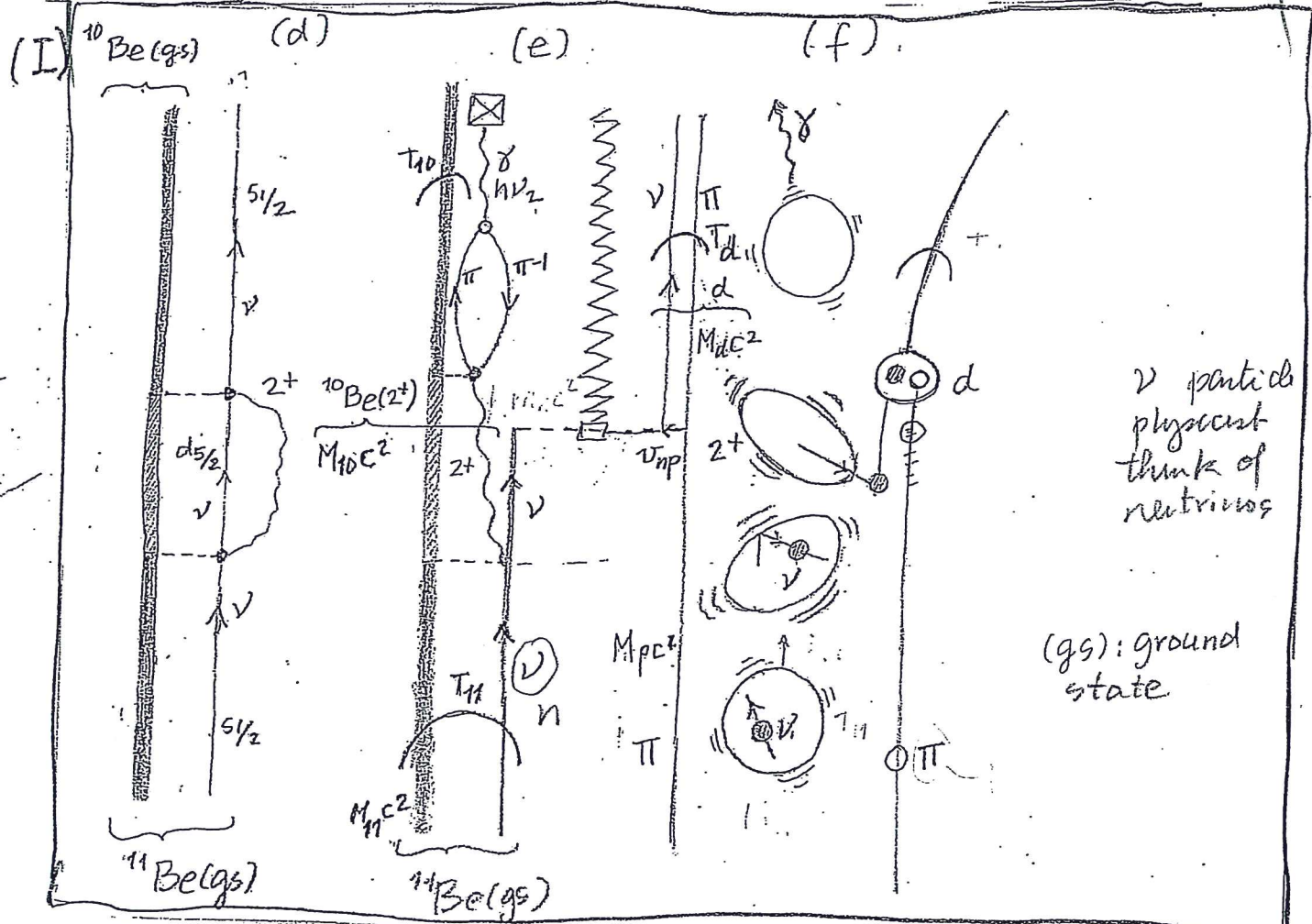
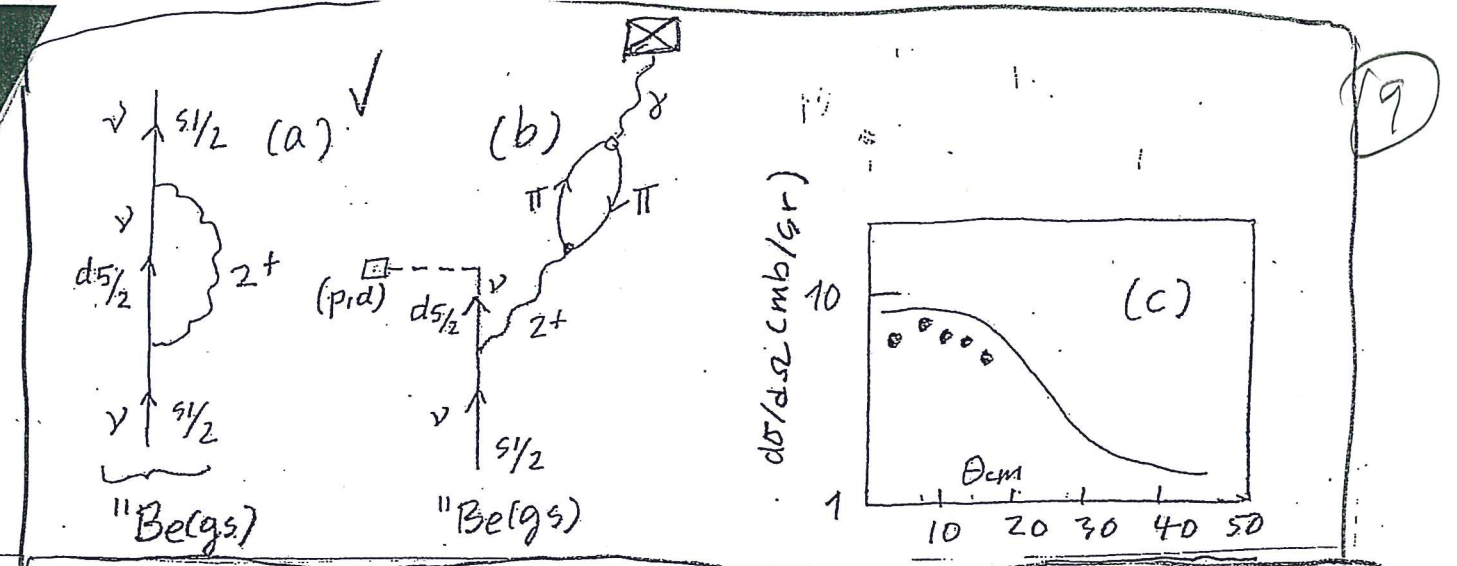
Fig. 6.2.1

(8)

62.1

Caption to Fig. 2

Bare (upper left (ul) thin horizontal lines) and dressed (bold face ul) single-particle levels of ^{11}Be . Due to the dressing of neutron motion with mainly quadrupole vibrations of the core ^{10}Be (insets (A) and (B)) inversion in sequence between the $2s_{1/2}$ and $1p_{1/2}$ levels (parity inversion) is observed. The numbers in parenthesis are energies in MeV. The Woods-Saxon (WS) mean field are indicated. In inset (C), low-energy levels of the hydrogen atom are indicated as well as the Coulomb field (Coul.). The effects of the spin-orbit coupling and Lamb shift associated with the splitting of the $2s_{1/2}$ and $2p_{1/2}$ level are displayed.



Caption to Fig. 6, 2, 2

Caption

(10)

- (I) NFT(r+s) diagram describing the reaction ${}^1\text{H}({}^{11}\text{Be}, {}^{10}\text{Be}(2^+, 3.368\text{MeV})) {}^2\text{H}$
- (II) ZPF of the ${}^{10}\text{Be}$ core and of the QED vacuum, connected with the spontaneous γ -decay of the $12^+; 3.368\text{MeV}$ state.



continues next page

Continuation caption

Fig. 6.2.2

(11)

In other words,

Caption to Fig. 3

(I) A virtual process in nuclear physics becomes real through the action of an external field. (a) Clothing process of the $1/2^+$ parity inverted ground state of $^{11}_4\text{Be}_7$ through the coupling to the low-lying quadrupole vibration of the core $^{10}_4\text{Be}_6$; the detailed structure of the NFT diagram is displayed in (d); (b) schematic representation of the pickup of the neutron moving around a $N = 6$ closed shell and populating the low-lying quadrupole vibrational state of this core, in coincidence with the corresponding γ -decay (see also II (f)) ; the detailed structure and reaction NFT diagram describing the pickup process in inverse kinematics, i.e. ${}^1\text{H}({}^{11}\text{Be}, {}^{10}\text{Be}(2^+, 3.368 \text{ MeV})) {}^2\text{He}$ is shown in (e) together with a cartoon representation in (f) (the jagged line represents a graphic mnemonic of the recoil effect, see [8] App. F as well as [27], App. A) ; (c) predicted (continuous curve) and experimental (solid dots) absolute differential cross sections associated with the pickup process. Proton and neutrons are labeled π and ν respectively, while d stands for deuteron. Curved arrows indicate projectile motion (reaction). Normal arrowed lines motion inside target or projectile (structure). (II) Interaction of protons in a nucleus with nuclear vibrations (solid dot, PVC vertex $\beta_L R_0 \partial U / \partial r Y_{LM}^*(\hat{r})$) [28], β_L : dynamical distortion parameter, $U(r)$ central potential) and photons (open circle, electromagnetic interaction $e \int d^4x J_\mu(x) A^\mu(x)$, A^μ being the vector potential, and J_μ the current density ($\mu = 1, \dots, 4$) [29]). While the variety of diagrams shown have general validity, we have assumed we are dealing with the low-lying correlated particle-hole quadrupole vibration ($L = 2$) of $^{10}_4\text{Be}_6$ lying at 3.37 MeV, its $B(E2; 0^+ \rightarrow 2^+) = 0.0052 e^2 b^2$ being associated with $\beta_2 \approx 0.9$. An arrowed line pointing upward (downward) describes a proton (proton hole) moving in the $p_{1/2}$ ($1p_{3/2}$) orbital. Zero point fluctuations of the nuclear ground state associated with : (a) the nuclear vibration, (b) the electromagnetic field associated with the corresponding spontaneous γ -decay. (c) Pauli principle correction to the simultaneous presence of the above two ZPF processes. (d) Intervening the virtual excitation of the nuclear vibrations (graph (c)) with an external (inelastic) field (cross followed by a dashed line), in coincidence with the γ -decay (γ -detector, crossed box), the virtual process (c) becomes real. (e),(f) time ordering of the above process correspond to the two RPA contributions through backwardsgoing and forwardsgoing amplitudes [28] and subsequent γ -decay.

Structure and reactions of ^{11}Be : many-body basis for single-neutron halo

F. Barranco,¹ G. Potel,² R.A. Broglia,^{3,4} and E. Vigezzi⁵

¹Departamento de Física Aplicada III, Escuela Superior de Ingenieros, Universidad de Sevilla, Camino de los Descubrimientos, Sevilla, Spain

²National Superconducting Cyclotron Laboratory, Michigan State University, East Lansing, Michigan 48824, USA

³The Niels Bohr Institute, University of Copenhagen, DK-2100 Copenhagen, Denmark

⁴Dipartimento di Fisica, Università degli Studi Milano, Via Celoria 16, I-20133 Milano, Italy

⁵INFN Sezione di Milano, Via Celoria 16, I-20133 Milano, Italy

The exotic nucleus ^{11}Be has been extensively studied and much experimental information is available on the structure of this system. Treating, within the framework of renormalised nuclear field theory (NFT)_{ren} in both configuration and 3D-space, the mixing of bound and continuum single-particle (*sp*) states through the coupling to collective vibrations of the ^{10}Be core, as well as Pauli principle acting not only between the single valence particle explicitly considered and those participating in the collective states, but also between fermions involved in two-phonon virtual states dressing the single-particle motion, it is possible, to simultaneously and quantitatively account for the energies of the $1/2^+$, $1/2^-$ low-lying states, the centroid and line shape of the $5/2^+$ resonance, the one-nucleon stripping and pickup absolute differential cross sections involving ^{11}Be as either target or residual nucleus, and the dipole transitions connecting the $1/2^+$ and $1/2^-$ parity inverted levels as well as the isotopic shift of the charge radius, thus providing a unified and exhaustive nuclear structure and reaction characterisation of the many-body effects which are at the basis of this paradigmatic one-neutron halo system.

PACS numbers: 21.60.Jz, 23.40.-s, 26.30.-k

If neutrons are progressively added to a light normal nucleus the Pauli principle forces, when the core becomes saturated, the wavefunctions of the last neutrons to move out and form a misty halo cloud. The resulting system displays a radius much larger than predicted by systematics, a sequence of levels contradicting the regular shell structure, and low-energy dipole transitions of strength ranked among the largest ever observed. The description of light exotic neutron-rich nuclei constitutes a formidable test of the ability of theory to simultaneously and on par account for (time dependent) mean field and many-body effects of similar magnitude, in which the nuclear surface and thus surface vibrations, play an overwhelming role.

The nucleus ^{11}Be constitutes one of the best and most studied experimentally [1]-[8] and theoretically [9]-[25] examples of the melting of the $N = 8$ closed shell, substituted by the new $N = 6$ magic number, a phenomenon resulting from the parity inversion between the $1p_{1/2}, 2s_{1/2}$ levels. Less known, although not less important, is the conspicuous tendency to parity inversion, not fully materialised, displayed by the $(1p_{1/2}, d_{5/2})$ pair of levels.

Nuclear Field Theory, tailored after Feynman diagrammatic version of Quantum electrodynamics (QED), has been successfully employed to accurately describe, in many cases at the 10% or better error level, the nuclear structure of heavy (^{204}Pb [26], ^{209}Bi [27, 28], ^{211}Pb [29], ^{212}At [30]), medium heavy ($^{118}-^{122}\text{Sn}$ [31-33]) and light two-neutron halo nuclei (^{11}Li [34], ^{12}Be [13]) with predictions, also in this case, accurately confirmed by experiment [35, 36]. Strong of four decades of systematic application and development of NFT [37-39], we take up, in the present letter, the challenge of describing the structure of ^{11}Be and the transfer reactions involving this nucleus, and attempt at answering central questions regarding its exotic properties : a) Does it exist and if

so, which is the mean field leading to the bare single-particle elementary modes of excitations which upon being dressed by vibrations, leads to the observed sequence of levels? b) Is there a universal mechanism at the basis of parity inversion and in the affirmative, has it been observed in other physical systems than the atomic nucleus? c) Which is the role played by many-body effects involving continuum states, regarding both resonances and single-particle transfer processes?

In the calculations discussed in this letter, we have simultaneously dealt with the $p_{3/2}, p_{1/2}, s_{1/2}$ and $d_{5/2}$ single-particle states up to an energy $E_{cut} = 25$ MeV, imposing vanishing boundary conditions at $R = 50$ fm (continuum discretization), treating their interweaving with the quadrupole collective vibrations of the ^{10}Be core (Suppl. Mat., Sect. 2) and taking into account the mixing between bound and continuum states. The same calculations have been repeated including also the octupole and the pair removal modes of the core ^{10}Be (see Suppl. Mat., Section 2 and 3), obtaining very similar results, and no physical effect not already found within the quadrupole vibration subspace. (in connection with the simultaneous treatment of particle-hole and pairing vibrations see also [45, 46]).

There are in all four parameters entering the calculations discussed in this letter (the depth V_0 , the radius R_0 , the diffusivity a and the spin-orbit strength $(V_{ls})_0$) which are allowed to vary freely in an attempt to determine the bare potential making use of an effective mass ($m_k = 0.7m(0.91m)$ for $r=0(\infty)$), see Suppl. Mat., Sect. 1, and two experimental (empirical) inputs, namely the excitation energy $\hbar\omega_2$ (= 3.368 MeV) and the dynamical deformation $\beta_2''(\approx 0.9)$, which characterize the low-lying quadrupole vibration of the core $^{10}\text{Be}_6$. The large value of β_2'' (see Suppl. Mat., Sect. 2), underscores the fact that the system is close to a quadrupole shape phase transition, a phenomenon closely connected with α -clustering in a light nucleus like ^{10}Be .

6.2.3

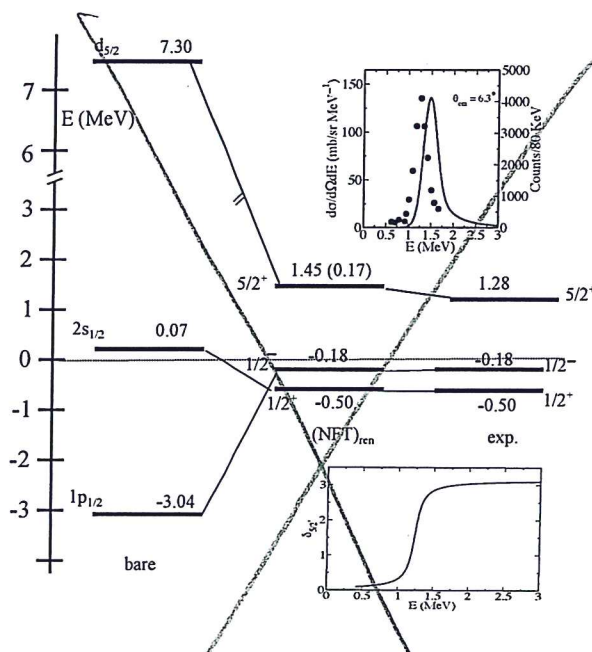


FIG. 1. Low-lying spectrum of ^{11}Be : (bare) unperturbed single-particle levels, solution of the bare mean field (see Suppl. Mat., Sect 1); $((\text{NFT})_{\text{ren}})$ dressed levels; (exp.) experimental values. The number on each thick horizontal line gives the energy of the state in MeV. The number in brackets correspond to the width of the $5/2^+$ resonance derived from the calculated elastic phase shifts (see inset on the lower right hand side). No phase shift data exist for this state, the 100 keV width often quoted being extracted from the ${}^9\text{Be}(\text{t},\text{p}){}^{11}\text{Be}(5/2^+)$ reaction ([41], Table 11.5). The line shape of the $5/2^+$ resonance calculated from the $(d^2\sigma/d\theta dE)_{\theta=6.3^\circ}$ (${}^{10}\text{Be} \rightarrow {}^{11}\text{Be}(5/2^+)$) strength function is displayed in the upper right hand side corner inset (continuous line) in comparison with the data (solid dots) [6].

Because of spatial quantization, the above scheme involves both energies and single-particle radial wave functions, in particular that of the $d_{5/2}$ resonance. The variety of many-body clothing processes lead to important modifications of these radial wave functions, and thus of the corresponding one-particle transfer form factors and escape particle wave functions, accounting for up to 50% changes in the value of the one-nucleon transfer absolute cross sections and of the $5/2^+$ resonance decay width, in overall agreement with experimental data. Important information concerning the nature of the $5/2^+$ resonance, and of the role the quadrupole mode plays in dressing the nucleons moving around the Fermi surface is provided by the reactions ${}^{10}\text{Be}(\text{d,p}){}^{11}\text{Be}(5/2^+, 1.783 \text{ MeV})$ and ${}^{11}\text{Be}(\text{p,d}){}^{10}\text{Be}(2^+; 3.368 \text{ MeV})$ which forces, in this last case, a virtual state to become observable. A fact that aside from shedding light on retardation mechanisms in clothing processes, implies that particle-vibration coupled intermediate states which dress the single-particle states have to be real states concerning both energy and amplitude, as well as radial shape. Thus, $((\text{NFT})_{\text{ren}}$ ([39] and refs. therein; see also [33, 37, 40]) is not a calculational ansatz but a quantal requirement. Within this context, it is of notice that self consistency

*) [39] [33, 37, 40]

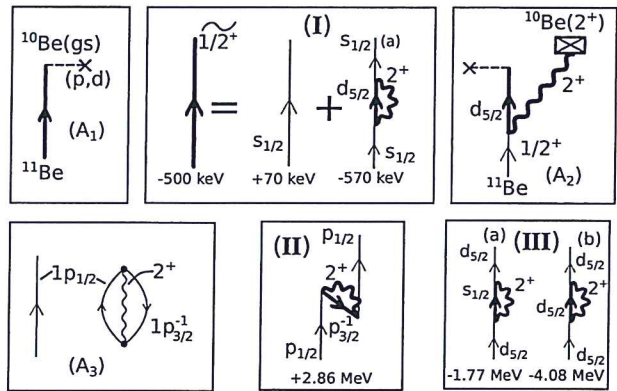


FIG. 2. $((\text{NFT})_{\text{ren}})$ diagrams describing the renormalization processes responsible for the different components of the clothed states (Eqs. (1)-(3)) associated with (I)-(III)) and the pickup processes populating the ground (A_1) and the first excited 2^+ state (A_2) of ${}^{10}\text{Be}$. (A_3) Valence nucleon in presence of a virtual zero point fluctuation of the core ${}^{10}\text{Be}$. Bold (thin) arrowed lines pointing upwards (downwards), describe dressed (bare) particle (hole) states. The wavy line represents the quadrupole vibration. A cross followed by a horizontal dashed line stands for an external one-neutron pickup (p,d) field. A crossed box indicates a detector, revealing the γ -ray associated with the eventual decay of ${}^{10}\text{Be}$.

6.2.1

within $((\text{NFT})_{\text{ren}})$ implies that the renormalized $\tilde{\epsilon}_j$ and $\tilde{\phi}_j(r)^{(i)}$ quantities reproduce the empirical input used for the intermediate states, while initial states (energies and wave functions) of the different graphical contributions are solutions of the bare potential (Fig. 1). In other words, for each value of $\tilde{\epsilon}_j$ there can exist more than one radial function, depending on whether the nucleon is moving around the ground state ($i = \text{gs}$) or around an excited state ($i = \text{coll}$) of the core, respectively. Technically, $\tilde{\phi}_j(r)^{(i)}$ are the form factors associated with stripping and pickup reactions around closed shells. For simplicity we will drop the superscript i in what follows.

Making use of the $((\text{NFT})_{\text{ren}})$ framework we have calculated the variety of self energy diagrams, renormalizing selfconsistently through the coupling to-quadrupole vibrations, the motion of the odd neutron of ${}^{11}\text{Be}$ in both configuration- (Fig. 2) and conformational 3D-space (Fig. 3). The dressed states associated with a given quantum number result from the iterative diagonalization of the particle-vibration coupling (PVC) Hamiltonian in a space composed of single-particle and of particle-phonon states, making use of self-energy function techniques (Fig. 2(I), see also Suppl. Mat., Section 4). The resulting states can be written as

$$|1/2^+\rangle = \sqrt{0.80}|s_{1/2}\rangle + \sqrt{0.20}|(d_{5/2} \otimes 2^+)_{1/2^+}\rangle \quad (1)$$

$$|1/2^-\rangle = \sqrt{0.84}|p_{1/2}\rangle + \sqrt{0.16}((p_{1/2}, p_{3/2}^{-1})_{2^+} \otimes 2^+)_{0+}, p_{1/2}\rangle \quad (2)$$

$$|5/2^+\rangle = \sqrt{0.49}|d_{5/2}\rangle + \sqrt{0.23}((s_{1/2} \otimes 2^+)_{5/2^+}\rangle \\ + \sqrt{0.28}|(d_{5/2} \otimes 2^+)_{5/2^+}\rangle. \quad (3)$$

The bare energies ϵ_j and the values $((\text{NFT})_{\text{ren}}) \tilde{\epsilon}_j$ associ-

one has
6.2.3

14

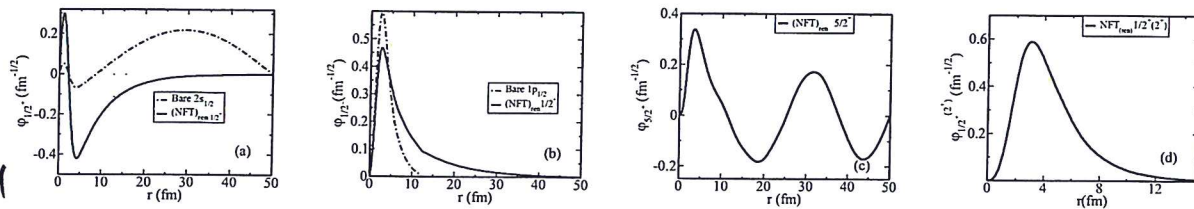


FIG. 9. Form factors of the $1/2^+$ (a), $1/2^-$ (b), $5/2^+$ (c) states and (d) the form factor associated with the reaction $^{11}\text{Be}(\text{p},\text{d})^{10}\text{Be}(2^+)$ calculated within the framework of $(\text{NFT})_{ren}$ ($a_{1/2^+} = \sqrt{0.80}$, $a_{1/2^-} = \sqrt{0.84}$, $a_{5/2^+} = \sqrt{0.49}$, $a_{(d_{5/2} \otimes 2^+)_{1/2^+}} = \sqrt{0.20}$, see Eqs. (1-3)). Also shown in (a) and (b) are the wave functions calculated with the bare potential (see also Suppl. Mat., Section 9).

6.2.1

ated with the renormalised single-particle states are shown in Fig. 6 in comparison with the experimental data. The corresponding wavefunctions $\phi_j(r)$ and $\tilde{\phi}_j(r)$ are displayed in Fig. 3. Concerning the bare potential leading to ϵ_j and $\phi_j(r)$, we refer to Suppl. Mat., Sect. 1. As seen from Fig. 1 there, the bare states are essentially equal to the HF solution of the SGH-Skyrme interaction. The most conspicuous effect emerging from NFT results is the reduction (in absolute value) of the energy difference between positive and negative parity states (Fig. 1): a factor of ten in the case of $1/2^-$, $1/2^+$ states and of six in the case of $5/2^+$, $1/2^-$ states. While parity inversion is only observed in the first case, the second had a close call.

Let us start by discussing the properties of the $5/2^+$ resonance. This state is prone to acquire a dynamical quadrupole moment (reorientation effect). This is because the particle-vibration coupling of the $d_{5/2}$ with itself (Fig. 2 (III)(b)) through the excitation of the quadrupole vibration of ^{10}Be , involves a rather confined single-particle resonant state radial wave function (Fig. 3 (c)). It results in a large (absolute) value of the associated PVC matrix element leading to an amplitude of $\sqrt{0.28}$ for the many-body component $|(\bar{d}_{5/2} \otimes 2^+)_{5/2^+}\rangle$ of the $|5/2^+\rangle$ state (Eq. (3)). An equally important component ($\approx \sqrt{0.23}$) is associated with the coupling of the $5/2^+$ state to the $s_{1/2}$ state, again through the quadrupole mode (Fig. 2(III)(a)). This coupling allows the bare $d_{5/2}$ resonance ($\epsilon_{5/2^+} \approx 7.3$ MeV, Fig. 1), to explore halo-like regions of the system and to lower its kinetic energy. Overall, these couplings result in an energy decrease of the $5/2^+$ strength and in the buildup of a narrow resonance with centroid at $E = 1.45$ MeV and a width of 170 keV as calculated from elastic scattering phase shifts (see lower left hand side inset, Fig. 1 and Suppl. Mat., Sect. 4). In turn, the $2s_{1/2}$ wave function mixes with the $(d_{5/2} \otimes 2^+)$ configuration and acquires a component of sizable amplitude ($\approx \sqrt{0.20}$, Eq. (1)) lowering, in the process, its bare energy by about 570 keV (Fig. 2 (I)(a)) and getting bound by 0.5 MeV. In other words, the $d_{5/2}$ state plays, through its coupling to the 2^+ vibration of the core, an essential role in the $(1/2^-, 1/2^+)$ parity inversion phenomenon, by lowering the energy of the $s_{1/2}$ state conspicuously. The numbers quoted above also contain the renormalisation contribution of the Pauli correcting diagrams associated with the implicit presence of two-phonon states in intermediate, virtual

configurations. Otherwise, the corrections arising from the self energy processes shown in Fig. 2(I) and (III) would have been much too attractive (see Suppl. Mat., Sect. 6).

The zero-point fluctuations (ZPF) associated with the ^{10}Be core, arising from the quadrupole vibrations (Fig. 2(A3)) make virtual use of the $p_{1/2}$ single-particle state. The diagram displayed in Fig. 2 (II) properly treats this problem, namely the antisymmetry between the valence nucleon and those participating in the vibration. As a result, the phase space of the clothed $1p_{1/2}$ state becomes smaller than the bare one, its binding becoming weaker by about 3 MeV due to a rather conspicuous Lamb-shift like effect, of the order of 10% of the value of the Fermi energy. Over counting (bubble corrections) is, in the present case, negligible (see Suppl. Mat., Sect. 5).

The radial dependence of the many-body wavefunctions and the phonon admixture in single-neutron states can be probed by the one-neutron transfer reactions $^{10}\text{Be}(\text{d},\text{p})^{11}\text{Be}$ and $^{11}\text{Be}(\text{p},\text{d})^{10}\text{Be}(2^+)$, populating the low-lying $1/2^+$, $1/2^-$ and $5/2^+$ states of ^{11}Be and the first excited 2^+ state of ^{10}Be , and proceeding through the form factors displayed in Figs. 3(a)-(c) and Fig. 3(d) respectively. Concerning the latter, we remark that the asymptotic decay constant of the $d_{5/2}$ radial wave function $\tilde{\phi}_{1/2^+}(r)^{(2^+)}$ associated with the $2^+ \otimes d_{5/2}$ configuration admixed in the $1/2^+$ ground state of ^{11}Be displays a binding energy $\epsilon_{1/2^+} - \hbar\omega_{2^+} = -3.8$ MeV. This is a natural outcome of $(\text{NFT})_{ren}$ which, through PVC and Pauli mechanism, provides the proper clothing of the $d_{5/2}$ orbital so as to make it able "to exist" inside the $|s_{1/2}\rangle$ state as a virtual, intermediate configuration (Fig. 2(I)(a)). The associated asymptotic r -behaviour results from the coherent superposition of many continuum states, and its spatial dependence in the surface region (Fig. 3 (d)) can hardly be simulated by making use of a bound single-particle wavefunction of a properly parameterized single-particle potential (separation energy approximation, commonly used in the literature), outcome which is in agreement with the result of previous studies [3].

The $(\text{NFT})_{ren}$ form factors shown in Fig. 3 were used, together with global optical potentials [42, 43], to calculate the one-nucleon stripping and pickup absolute differential cross sections of the reactions mentioned above (see Suppl. Mat., Section 10). The results provide an overall account of the experimental findings (Fig. 4). Within this context we remark

Third

*) [42, 43]

4

6.2.4

6.2.4

6.2.3

6.2.3

6.2.5

6.2.3

6.2.4

that the pickup process shown in inset (A₁) of Fig. 2 and populating ¹⁰Be ground state implies the action of the external (p,d) field on the left hand side (lhs) of the graphical representation of Dyson equation shown in Fig. 2(I), and involves, at the same time, the use of the corresponding radial wavefunction as form factor (Fig. 3(a)). In the case of the population of the first 2⁺ excited state of ¹⁰Be (inset A₂), the (p,d) field acts on the $(d_{5/2} \otimes 2^+)_{1/2^+}$ virtual state of the second graph of the right hand side (rhs) of this equation (Fig. 2(I)(a)), involving this time the radial wave function $\phi_{1/2^+}(r)^{(2^+)}$ as form factor (Fig. 3(d)). Summing up, insets (A₁) and (A₂) and diagrams (I) of Fig. 2 testify to the subtle effects resulting from the unification of (NFT)_{ren} of structure and reactions discussed in [39], and operative in the cross sections shown in Fig. 4, as a result of the simultaneous-and-self-consistent treatment of configuration and 3D-space. Within this context the bold face drawn state $| (d_{5/2} \otimes 2^+)_{1/2^+} \rangle$ shown in Fig. 2(I)(a) and the radial wave function (NFT)_{ren} displayed in Fig. 3(d) can be viewed as *on par* structure and reaction-intermediate elements of the quantal process ¹¹Be(p,d)¹⁰Be(2⁺).

PVC leads also to important renormalization effects in the dipole-electromagnetic transitions of the system. This is due to the poor overlap between the renormalised halo radial wave functions and those of the core nucleons which screen the symmetry potential, impeding the GDR to shift the $1/2^+ \rightarrow 1/2^-$ single-particle E1-strength to high energies in the attempt to exhaust the EWSR [44]. The strength of the dipole transition calculated making use of the dressed states lead to $B(E1; 1/2^- \rightarrow 1/2^+) = 0.11 e^2 fm^2$, a value to be compared to the experimental value $B(E1) = 0.102 \pm 0.002 e^2 fm^2$ [8]. No free parameters were used in the calculations (for details see Suppl. Mat. Sect. 6).

We now discuss the isotopic shift of the charge radius (Suppl. Mat., Section 7). The corrections to $\langle r^2 \rangle_{^{10}\text{Be}}^{1/2}$ arising from the addition of a neutron are obtained applying the external field operator r^2 to the different particle and collective vibration lines of the diagrams appearing in the rhs of the graphical equation displayed in Fig. 2(I). The summed (recoil) contributions associated with the $s_{1/2}$ state ($\langle r^2 \rangle_{1/2^+}^{1/2} / 11 \rangle^2 (\langle r^2 \rangle_{1/2^+}^{1/2} = 7 \text{ fm})$ is to be multiplied by the square of the renormalised $|1/2^+\rangle$ state single-particle amplitude ($= 0.80$, Eq. (1)). Those associated with the $d_{5/2}$ and 2⁺ elementary modes appearing in the intermediate state of graph (a) of Fig. 2(I) lead to (recoil) ($\langle r^2 \rangle_{5/2^+}^{1/2} / 11 \rangle^2$ and (dynamical deformation) ($\langle r^2 \rangle_{5/2}^+ \beta_2^2 / 2\pi$) contributions respectively, and are to be multiplied by the square amplitude ($= 0.20$) associated with the $(d_{5/2} \otimes 2^+)_{1/2^+}$ configuration (Eq. (1)). The resulting theoretical prediction $\langle r^2 \rangle_{^{11}\text{Be}}^{1/2} = 2.48 \text{ fm}$, accurately reproduces the experimental finding $2.44 \pm 0.06 \text{ fm}$ [7].

We conclude that the existence of a bare potential and associated k -mass whose eigenstates essentially coincide with the HF-solution of SGII Skyrme interaction, forcefully testifies to the validity of mean-field approaches in the description of light halo nuclei in general, and ¹¹Be in particu-

lar. The fact that a substantial fraction of the low-lying single-particle states, as much as 50% in the case of the $d_{5/2}$ state, corresponds to many-body configurations as well as the strong Pauli principle repulsion associated with two-quadrupole phonon virtual states dressing single-particle motion, testifies equally forcefully to the time-dependent nature of the mean field, let alone the strong anharmonic character of this dependence.

Parity inversion results mainly from Pauli blocking of the ground state (quadrupole) zero-point fluctuations of the core ¹⁰Be by the odd $p_{1/2}$ neutron, together with the dressing of the $s_{1/2}$ state by the same vibration. The physics at the basis of this phenomenon has been observed for the first time in the spectrum of hydrogen atom by Lamb and coworkers [47, 48]. The Lamb shift, that is the fact that the $2s_{1/2}$ level of H lies higher than the $2p_{1/2}$ by 1058 MHz (4.4 μeV) while Dirac equation predicts them to be degenerate, provided the first measure of QED vacuum fluctuations. Within the context of nuclear physics, one can mention that the relative "large" upshift (+129 keV) of the $I = 15/2^+$ member of the $(h_{9/2}(\pi) \otimes 3^- ({}^{208}\text{Pb}))_I$ septuplet of ²⁰⁹Bi, one of the first experimental tests to which NFT was subject, has the same origin as the 2860 keV upshift of the $p_{1/2}$ level of ¹¹Be.

At the basis of the large magnitude of the renormalization effects observed in ¹¹Be, one finds a fundamental parameter of NFT, namely the effective degeneracy $\Omega (\approx 2/3 A^{2/3})$ of the single-particle phase space, $1/\Omega$ being the small expansion parameter. In the case of ¹¹Be, Ω is rather small (≈ 3) as compared with heavy nuclei like e.g. ²⁰⁹Bi ($\Omega \approx 24$), a fact which underscores the need to sum to all orders (in $1/\Omega$) those processes operative in the dressing of single-particle states. Furthermore, in the case of ¹¹Be, the surface (S) to volume (V) ratio ($r = aS/V$, a being the diffusivity) is much larger (≈ 0.74) than in the case of heavy nuclei lying along the stability valley (≈ 0.28 in the case of ²⁰⁹Bi).

Finally one can posit that the renormalization of the radial dependence of the single-particle states due to the many-body processes involving the continuum states plays an important role in the absolute one-nucleon transfer differential cross sections.

Acknowledgment

F.B and E.V. acknowledge funding from the European Union Horizon 2020 research and innovation program under Grant Agreement No. 654002.

-
- [1] H. Iwasaki *et al.*, Phys. Lett. B **481** (2000) 7
 - [2] S. Fortier *et al.*, Phys. Lett. B **461** (1999) 22
 - [3] J.S. Winfield *et al.*, Nucl. Phys. A **683** 48 (2001)
 - [4] D.L. Auton, Nucl. Phys. A **157**, 305 (1970)
 - [5] B. Zwieglinski *et al.*, Nucl. Phys. A **315**, 124 (1979)
 - [6] K.T. Schmitt *et al.*, Phys. Rev. C **88** (2013) 064612
 - [7] W. Nörterhäuser *et al.*, Phys. Rev. Lett. **102** (2009) 062503

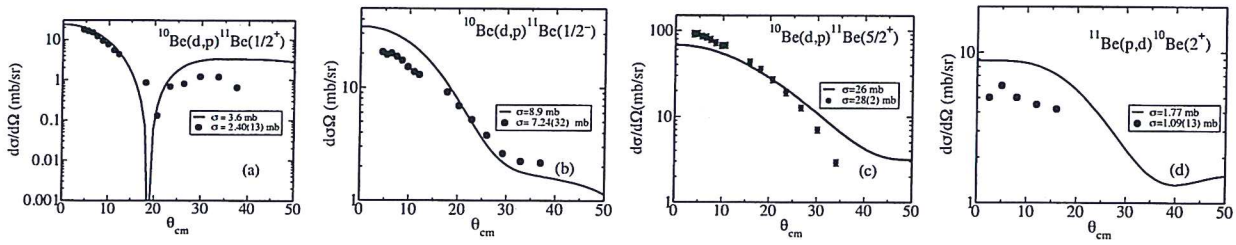


FIG. 4. (a-c) (continuous curve) Absolute differential and (insets) summed cross sections associated with the reactions ${}^2\text{H}({}^{10}\text{Be}, {}^{11}\text{Be}){}^1\text{H}$ at $E=107$ MeV, populating the $1/2^+$, $1/2^-$, and $5/2^+$ states. The experimental data [6] are displayed in terms of solid dots. (d) Same as before, but for the reaction ${}^1\text{H}({}^{11}\text{Be}, {}^{10}\text{Be}){}^2\text{H}$ at $E=388.3$ MeV, populating the 2^+ state [3].

- [8] E. Kwan *et al.*, Phys. Lett. **B732** (2014) 210
- [9] I. Talmi and I. Unna, Phys. Rev. Lett. **4**, 469 (1960)
- [10] T. Otsuka, N. Fukunishi, and H. Sagawa, Phys. Rev. Lett. **70** (1993) 1385
- [11] H. Sagawa, B. A. Brown, and H. Esbensen, Phys. Lett. B **309** (1993) 1
- [12] N. Vinh Mau, Nucl. Phys. **A592** (1955) 33
- [13] G. Gori, F. Barranco, E. Vigezzi and R.A. Broglia, Phys. Rev. C **69** (2004) 041302(R)
- [14] F.M. Nunes, I.J. Thompson and R.C. Johnson, Nucl. Phys. **A596** (1996) 171
- [15] K. Fossez, W. Nazarewicz, Y. Jaganathan, N. Michel, and M. Ploszajczak, Phys. Rev. C **93** (2016) 011305(R)
- [16] I. Hamamoto and S. Shimoura, J. Phys. **G34** (2007) 2715
- [17] Y. Kanada-En'o and H. Horiuchi, Phys. Rev. C **66** (2002) 024305
- [18] A. Calci, P. Navrátil, R. Roth, J. Dohet-Eraly, S. Quaglioni and G. Hupin, Phys. Rev. Lett. **117** (2016) 242501
- [19] A. Krieger *et al.*, Phys. Rev. Lett. **108** (2012) 142501
- [20] N.R. Timofeyuk and R.C. Johnson, Phys Rev. C **59** (1999) 1545
- [21] N. Keeley, N. Alamanos and V. Lapoux, Phys. Rev. C **69** (2004) 064604
- [22] A. Deltuva, Phys. Rev. C **79** (2009) 054603
- [23] A. Deltuva, Phys. Rev. C **88** (2013) 011601(R)
- [24] J.A. Lay, A.M. Moro, J.M. Arias and Y. Kanada-En'yo, Phys. Rev. C **89** (2014) 014333
- [25] R. de Diego, J.M. Arias, J.A. Lay, A.M. Moro, Phys. Rev. C **89** (2014) 064609
- [26] P.F. Bortignon *et al.*, Phys. Lett. **76B** (1978) 153
- [27] P.F. Bortignon *et al.*, Phys. Rep. **30C** (1977) 305
- [28] A. Bohr and B.R. Mottelson, *Nuclear structure*, Vol. II , Benjamin, Mass (1975)
- [29] O. Civitarese *et al.*, Phys. Lett. **72 B** (1977) 45
- [30] F.A. Janouch *et al.*, Phys. Lett. **82B**, (1979) 329
- [31] A. Idini, Ph.D., University of Milano, unpublished
- [32] A. Idini, F. Barranco and E. Vigezzi, Phys. Rev C **85** (2012) 014331
- [33] A. Idini *et al.*, Phys. Rev. C **92** (2015) 031304(R)
- [34] F. Barranco *et al.*, Eur. Phys. J. (2001) F. Barranco, P.F. Bortignon, R.A. Broglia, G. Colò and E. Vigezzi, Eur. Phys. J. A **11**, 385 (2001)
- [35] I. Tanihata *et al.*, Phys. Rev. Lett. **100**, 192502 (2008)
- [36] G. Potel, F. Barranco, E. Vigezzi and R.A. Broglia, Phys. Rev. Lett. **105** (2010) 172502
- [37] D.R. Bes *et al.*, Nucl. Phys. **A293** (1977) 350
- [38] D.R. Bes and J. Kurchan, *The Treatment of Collective Coordinates in Many-Body Systems*, World Scientific (1990)
- [39] R.A. Broglia, P.F. Bortignon, F. Barranco, E. Vigezzi, A. Idini and G. Potel, Phys. Scr. **91** (2016) 063012
- [40] R.D. Mattuck, *A guide to Feynman diagrams in the many-body problem*, Dover, New York (1976)
- [41] J.H. Kelley *et al.*, Nucl. Phys. A **880** (2012) 88
- [42] Y. Han, Y. Shi and Q. Shen, Phys. Rev. C **74** 044615 (2006)
- [43] J. Konig and J.-P. Delaroche, Nucl.Phys. A **713** (2003) 231
- [44] P.F. Bortignon, A. Bracco and R.A. Broglia, *Giant resonances*, Harwood Academic Publishers , Amsterdam (1998)
- [45] W.H. Dickhoff and D. Van Neck, *Many-body theory exposed! : Propagator description of quantum mechanics in many-body systems*, World Scientific (2008)
- [46] C. Barbieri and W.H. Dickhoff, Phys. Rev. C **68** (2003) 014311
- [47] W.Lamb and R. Rutherford, Phys. Rev. **72** (1947) 241
- [48] N.M. Kroll and W.E. Lamb, Phys. Rev. **75** (1949) 388

(17)

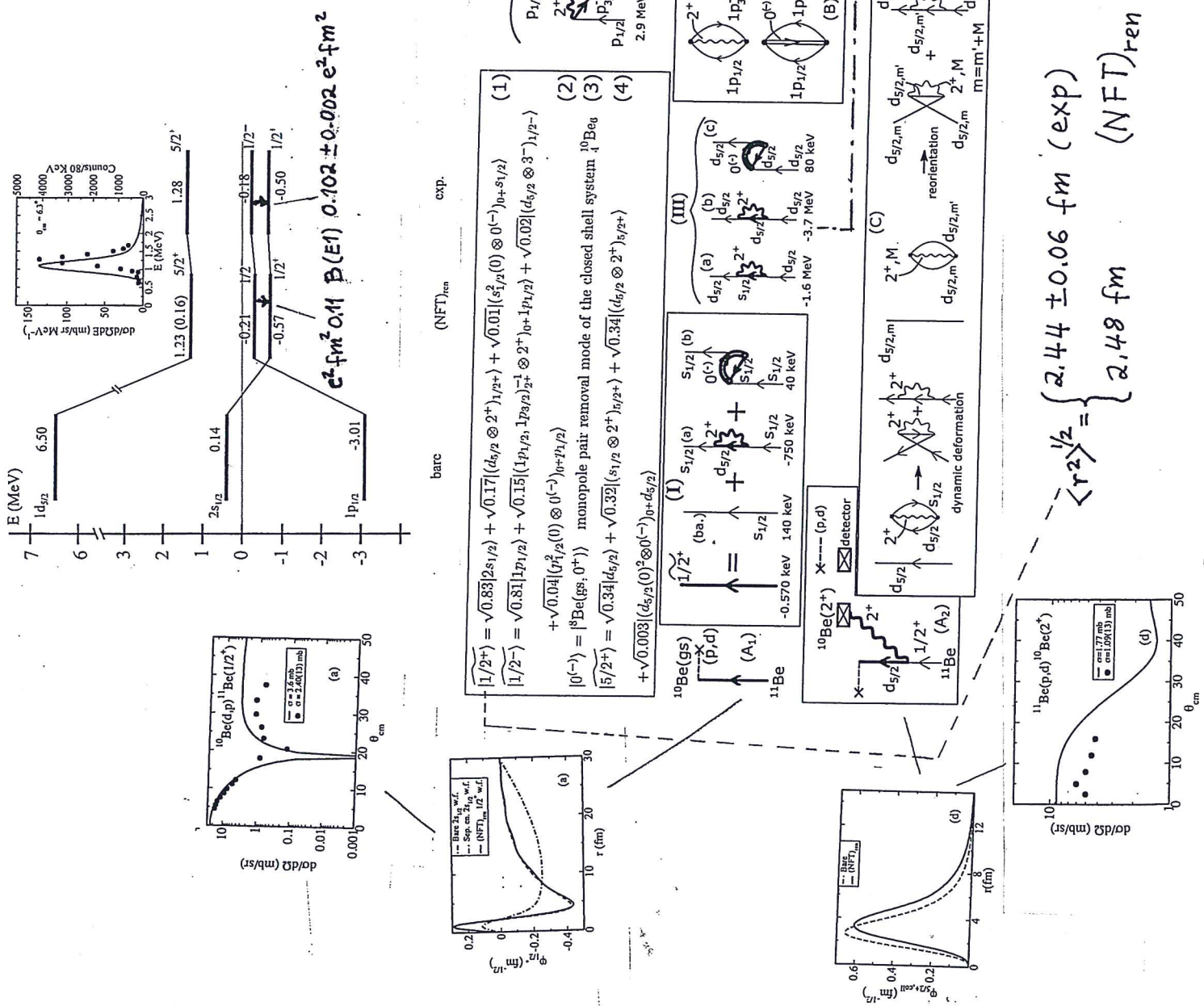


Fig. 6.3.1 ^{11}Be single page

(18)

The clothing of the bare nucleons (single arrowed thin lines) with quadrupole and octupole particle-hole and monopole pair removal vibrations of the ^{10}Be core following the rules of renormalized nuclear field theory, give rise to values of the (renormalized) energies \tilde{E}_j in ~~overall~~ agreement with observation and to renormalized single-particle wavefunctions $\tilde{\phi}_j$ which used as formfactors in connection with optical potentials provide an overall account of the absolute ~~and~~ and nucleon stripping and pickings differential cross sections. The same is true concerning the $B(E1)$ transition between the parity inverted $1/2^+, 1/2^-$ states and the charge radius.